32. Barber, J. (ed.) *The Photosystems: Structure Function and Molecular Biology* (*Topics in Photosynthesis Vol.* 11) (Elsevier, Amsterdam, 1992).
33. Roelofs, T. A., Gilbert, M., Schuvalov, V. A. & Holzwarth, A. R. *Biochim. biophys. Acta* **1060,** 237–244 (1991).
34. Holzwarth, A. R. *Photochem. Photobiol.* **43,** 707–725 (1986).
35. Falkowski, P. G., Kolber, Z. & Mauzerall, D. *Biophys. J.* **66,** 923–925 (1994).

ACKNOWLEDGEMENTS. We thank H. Walker and E. Green for helping to arrange this collaborative effort, Z. Johnson, P. Chisholm, J. Berges and D. Wallace for constructive suggestions in preparation of the manuscript, and T. Stanton for help with the colour graphics. This research wass supported by the US DoE, the US EPA, NASA and the US Office of Naval Research.

Seismic anisotropy and mantle flow beneath the Baikal rift zone

S. Gao*, P. M. Davis*, H. Liu*, P. D. Slack*, Yu. A. Zorin† V. V. Mordvinova†, V. M. Kozhevnikov† & R. P. Meyer‡

* Department of Earth and Space Sciences, University of California, Los Angeles, California 90024, USA
† Institute of the Earth's Crust, Russian Academy of Sciences, Irkutsk 664 033, Russia
‡ Department of Geology and Geophysics, University of Wisconsin, Madison, Wisconsin 53706, USA

SEISMIC studies have shown that continental rifts such as Lake Baikal and the Great Rift Valley of East Africa are like mid-ocean rifts in that they lie above broad regions of asthenospheric upwarp of much greater extent than the surface expression of rifting[1–4]. The direction of mantle flow in such regions can be investigated using the seismic anisotropy created by flow-induced orientation of mantle olivine crystals[5–8]. Seismic studies of the Mid-Atlantic Ridge have revealed upwelling mantle flow beneath the ridge and flow normal to the ridge axis on either side[8–10]. Here we present results from an array of seismic stations across the Baikal rift zone in southern Siberia. The splitting in arrival times of SKS seismic waves indicates that the upper mantle beneath the rift zone is anisotropic, with the fast direction (which reflects the direction of mantle flow) being horizontal and normal to the rift axis. This suggests that the broad upwarp associated with this continental rift is caused by similar mantle flow to that at mid-ocean rifts. This may help to elucidate the processes involved in continental rifting.

Rifting at Baikal began ~30 million years ago at an early stage of the collision between India and Eurasia[11]. Molnar and Tapponnier[12] have suggested that the India–Asia collision generated most of the large-scale tectonics of Asia, and that the collision perhaps ripped open Lake Baikal more than 3,000 km away. In eastern Mongolia and China these authors note that deformation takes place in a shear zone of east–west, left lateral, strike-slip faults. They suggest that Baikal rifting results from a mechanism equivalent to the development of tension cracks near the ends of, and oblique to, shear zones. The diagrams in the upper-right corner of Fig. 1 show that if mantle flow beneath Lake Baikal is orthogonal to the rift[9,13], then the fast direction on the flanks would also be orthogonal to the rift, that is, in a northwest–southeast direction. On the other hand, as shown by the upper diagram, if rifting is a pull-apart structure within a regional shear zone[12], and this was the only motion orientating mantle olivine, the fast direction would not be orthogonal to the rift, and would most likely be east–west, because this is the direction of strain associated with the opening of the rift.

Anisotropy of the mantle is readily detected by birefringent effects on SKS phases from distant earthquakes[14–21]. When the upward-travelling shear wave encounters anisotropic material, it may split into shear waves with two polarizations with different velocities, denoted fast and slow. The difference in arrival time between the fast and slow directions, which can amount to seconds, quantifies the degree of splitting.

In the summer of 1992 we installed 28 three-component seismic stations along the profile across the Baikal rift zone shown in Fig. 1. During the 3.5-month recording period, 9 events were found to be suitable for studying SKS phases (that is, strong events with epicentral distances >82° from the mid-point of the profile; Table 1) We have found that the effect of anisotropy can be distinguished provided the back-azimuth differs from the fast or slow directions by >10°. Although the events have a narrow range of back-azimuths (111–122°), most measurements satisfy this criterion. Figure 2 shows some seismograms with the split arrivals. We determine the two splitting parameters, fast polarization direction and splitting time, by searching for the minimum of an error function[21]. The radial and transverse components are rotated into candidate fast and slow directions, and the slow component advanced in time to be in phase with the fast component. For optimal parameters

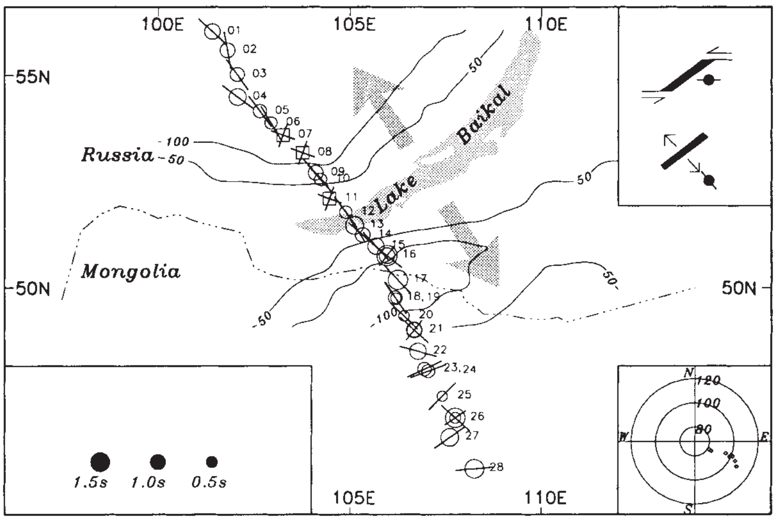

FIG. 1 Map showing the region with the stations of the seismic array extending from the Siberian platform across the Baikal rift zone into Mongolia. Stations with well defined measurements are represented by single circles with size proportional to the splitting (see lower-left corner). The line drawn through each circle gives the fast polarization direction. Those with two inconsistent results are plotted as double circles. The shorter and longer line indicates the fast direction of the smaller and larger circle, respectively. Stations represented by squares are those on which anisotropy effects cannot be clearly observed. Contour lines are thickness of subcrustal lithosphere in kilometres, compiled from previous studies[4,25]. Arrows are direction of extensional stress from the generalized global stress map of Zoback[22]. Stations 01, 11 and 28 had broadband sensors (STS-2) and the rest employed short-period sensors with central frequencies 0.5–2 Hz. During the experiment two stations (18 and 23) were relocated to nearby new sites (19 and 24). The resulting splitting parameters at old and new stations are similar. The schematic diagrams in the the upper-right corner show two possibilities for the formation of the Baikal rift. Top, pull-apart basin from an east–west left lateral shear. The anisotropy symbol shows that the expected fast direction is in the shear direction east–west. Numerical simulations[28] indicate that almost complete alignment of olivine crystals occurs for strain >0.4. Bottom, upwelling flow in the mantle spreads out laterally from the rift. The expected fast direction is northwest–southeast. The polar plot in the the lower-right corner gives the back-azimuths and epicentral distances of the earthquakes relative to station 13 (see Table 1).

TABLE 1 Seismic events used in this study

Event no.	Date	Origin time (UT 1992)	Coordinates Lat. (°)	Long. (°)	Depth (km)	m_b^*	Distance† (°)	Back-az† (°)
1	25 Jun	06:30:51.2	−28.063	−176.735	18	6.1	104.60	116.65
2	26 Jun	03:18:54.0	−33.682	−179.076	33	5.6	107.65	121.97
3	11 Jul	10:44:20.9	−22.284	−178.507	381	6.2	99.10	114.27
4	4 Aug	06:58:35.8	−21.584	−177.322	278	5.7	99.22	112.96
5	4 Aug	21:08:44.0	−12.023	−166.496	109	5.9	82.46	119.97
6	25 Aug	08:24:13.7	−20.620	−175.151	67	5.5	99.73	110.75
7	30 Aug	20:09:06.9	−17.738	−178.775	573	5.8	95.36	111.69
8	10 Sep	10:43:20.4	−22.518	−175.052	39	5.5	101.26	111.87
9	15 Sep	21:04:00.9	−14.122	167.263	196	6.1	84.61	120.51

* Body-wave magnitude. † Relative to station 13.

superposition of the two components gives a linear variation (Fig. 2). The 95% confidence intervals are determined using the method proposed by Silver and Chan[21]. The final splitting parameters (Fig. 1, Table 2) are obtained by weighted averaging according to the 95% confidence interval of each individual measurement, and show the following.

(1) Beneath the rift zone and Siberian platform, most of the fast directions are northwest–southeast, that is orthogonal to the strike of the rift, and parallel to the extensional stress direction[22]. (2) At the transition to the fold belt in northern Mongolia, the fast direction changes to nearly east–west, that is parallel to the faulting and fold axis. (3) The transition takes place between stations 20 and 22, over a distance of 100 km. (4) The splitting ranges from 0.3 to 1.6 s with a mean value of 0.9 s which is consistent with a layer ~100 km thick characterized by 4% anisotropy. (5) Anisotropy effects cannot be resolved at stations 07, 08 and 11. At stations 16, 21 and 26, two sets of splitting parameters fit the data equally well. Therefore, both sets are presented. One of the two fast directions is consistent with neighbouring stations.

As SKS phases have a near-vertically-incident ray path, it is not possible to determine the depth of the anisotropic layer using values of splitting time alone. We use three approaches to constrain the depth. The first is aimed at determining how much of the anisotropy lies in the crust. It involves searching for anisotropy effects on P to S converted crustal phases[23]. The observed converted S-waves in our data show no effects of anisotropy. Therefore we conclude that the layer of anisotropy is in the mantle.

The second constraint on depth concerns the sudden transition in the fast directions from nearly east-west to northwest-southeast, which occurs between stations 20 and 22. We have calculated that for an anisotropy contrast at depth, the transition at the surface occurs over a scale length given by the inner Fresnel zone at that depth. Given that the wavelength of the SKS phase is 20 km, we calculate[24] that the associated Fresnel zone occurs at a depth of <250 km, that is, between the asthenosphere and the surface.

The third constraint suggests that the source is unlikely to be entirely in the subcrustal lithosphere. Estimates of subcrustal lithospheric thickness based on gravity, surface waves and teleseismic P-wave delays[4,25] range from 0 km along the rift axis to ~50 km in the regions 100 km each side of the rift axis (Fig. 1). At least in these regions, the subcrustal lithosphere is not thick

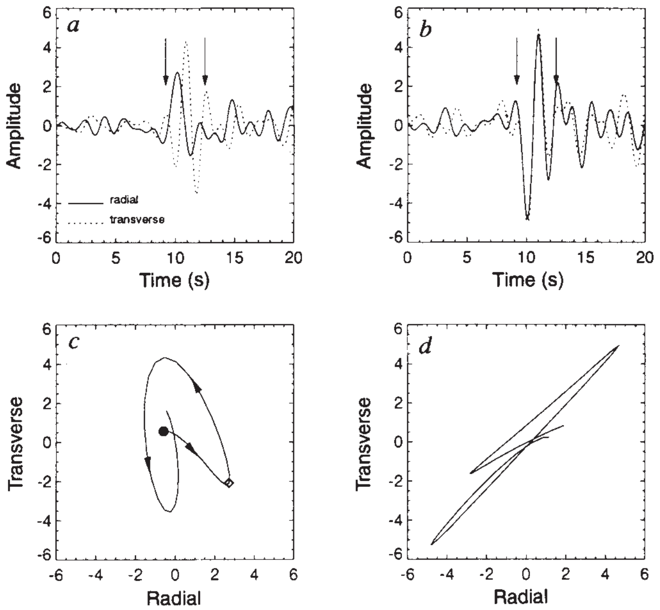

FIG. 2 Original and rotated horizontal components and particle motion patterns from event 7 for station 24. *a*, Original radial and transverse components. *b*, 'Isotropic SKS', that is, SKS arrival before entering anisotropic zone, constructed from fast and slow components, respectively. *c*, Particle motion pattern for the section between the two arrows in *a*. The arrival of the fast wave is labelled with a dot and that of the slow wave by a diamond. Arrows represent particle motion direction. *d*, Particle motion pattern for the section between the two arrows in *b*. The pattern is close to a straight line with 45° tilt angle.

TABLE 2 SKS splitting parameters and station locations

Station no.	Fast direction (°)	Splitting time (s)	Station lat. (°)	Station long. (°)	Event no.*
01	133 ± 07	1.0 ± 0.5	55.965	101.410	9
02	170 ± 13	0.9 ± 0.4	55.560	101.803	6
03	145 ± 03	0.8 ± 0.1	55.022	102.055	4, 5, 6, 7, 8
04	128 ± 04	1.2 ± 0.1	54.516	102.070	1, 2, 3, 4, 5, 6, 7, 8, 9
05	144 ± 03	0.7 ± 0.1	54.193	102.649	1, 2, 3, 6, 7, 8, 9
06	149 ± 09	0.6 ± 0.2	53.929	102.934	1, 7, 8
07a	110 ± 30	—	53.649	103.255	1, 2, 3, 7, 8
07b	020 ± 30	—	53.649	103.255	1, 2, 3, 7, 8
08a	110 ± 30	—	53.243	103.767	1, 2, 3, 7, 8
08b	020 ± 30	—	53.243	103.767	1, 2, 3, 7, 8
09	138 ± 05	0.9 ± 0.2	52.778	104.105	1, 2, 3
10	138 ± 07	0.6 ± 0.1	52.622	104.234	1, 2, 3, 4, 7, 8
11a	110 ± 30	—	52.169	104.469	7
11b	020 ± 30	—	52.169	104.469	7
12	144 ± 19	0.6 ± 0.4	51.847	104.893	2
13	148 ± 17	1.3 ± 0.3	51.526	105.121	8
14	132 ± 06	0.9 ± 0.3	51.292	105.339	6, 7, 8
15	138 ± 06	1.1 ± 0.1	51.021	105.682	1, 3, 7
16a	038 ± 04	1.0 ± 0.2	50.791	105.970	3, 7
16b	129 ± 07	1.6 ± 0.4	50.791	105.970	1, 6
17	137 ± 16	1.5 ± 0.4	50.193	106.254	6
18	145 ± 16	0.8 ± 0.1	49.747	106.188	4, 6, 7, 8
19	147 ± 24	0.3 ± 0.3	49.738	106.202	1, 2
20	134 ± 09	0.4 ± 0.2	49.288	106.412	1, 2, 3, 8
21a	039 ± 11	1.0 ± 0.4	48.931	106.682	2, 3
21b	132 ± 10	0.8 ± 0.6	48.931	106.682	1, 7
22	105 ± 06	1.1 ± 0.3	48.383	106.783	1, 2, 3, 7
23	064 ± 04	0.8 ± 0.1	47.921	106.954	1, 2, 3
24	069 ± 06	0.7 ± 0.1	47.866	107.051	4, 7, 8
25	044 ± 07	0.3 ± 0.1	47.209	107.422	3, 4, 7, 8
26a	056 ± 10	0.4 ± 0.1	46.635	107.758	4, 7
26b	132 ± 03	1.5 ± 0.2	46.635	107.758	3, 6, 8
27	055 ± 22	1.3 ± 0.3	46.115	107.619	4, 7, 8
28	085 ± 34	1.4 ± 0.6	45.262	108.260	3, 4, 6, 7, 8

* See Table 1.

enough to generate the observed 1-s splitting, unless the anisotropy is >10% which is unrealistic for subcrustal lithosphere. Therefore we conclude that, at least in the vicinity of the rift zone, the source of anisotropy is in the asthenosphere.

The fast direction for the southern part of the profile is roughly east–west. This may have been generated in a layer of mantle deformed by the collision of India and Asia. It could also be a relict from the ancient past. However, this fast direction is consistent with the dominant direction found across the Tibetan plateau[26]. Both the Tibetan and the Mongolia plateaus have been deformed by Cenozoic deformation related to the collision. The observed fast directions in both regions may have the same origin, that is, the continental collision.

Horizontal upper-mantle flow has previously been inferred using SKS splitting at six stations positioned along the axis of the Rio Grande rift[27] of the western United States. The mean splitting ranges from 0.9 to 1.5 s, with the fast directions being parallel or subparallel to the rift axis. The results were interpreted as being caused by the longitudinal component of a three-dimensional small-scale convection cell associated with the Rio Grande rift. Unfortunately, comparison of this earlier study with our results cannot readily be made as the Baikal rift stations were installed exclusively along a profile across the rift and not along it.

Thus, we suggest that the observed orientation of the anisotropy around Lake Baikal is the result of uppermost-mantle flow associated with recent tectonics. The results in the far south of the study region can be explained by the shear field associated with the collision of India and Asia, whereas those from either side of the Baikal rift reflect the rift's opening. Other studies[4,25] have shown that the asthenosphere upwarps in a broad zone extending either side of Lake Baikal, reaching the base of the crust at the lake itself. The inferred flow responsible for the upwarp is expected to remove ancient anisotropy. As at the mid-Atlantic rift, the fast direction on either side of the Baikal rift is normal to the rift axis. Measurements of vertical anisotropy along the Baikal rift axis will be required to identify whether upwelling mantle flow also occurs directly beneath the rift as is observed on the Mid-Atlantic Ridge[9]. Lithosphere thinning caused by mantle flow would produce a zone of inherent weakness. This can explain how the stresses from the collision of India and Asia could have induced Baikal rifting[12] at such a great distance from the zone of collision. □

Received 20 May; accepted 29 July 1994

1. Parker, E. C., Davis, P. M., Evans, J. R., Iyer, H. M. & Olsen, K. H. *Nature* **312**, 354–356 (1984).
2. Davis, P. M. *Tectonophysics* **197**, 309–325 (1991).
3. Zorin, Yu. A. *Tectonophysics* **73**, 91–104 (1981).
4. Gao, S. *et al. J. geophys. Res.* **99**, 15319–15330 (1994).
5. Babuska, V. & Cara, M. *Seismic Anisotropy in the Earth* (Kluwer, Dordrecht, 1991).
6. Vinnik, L. P., Makeyeva, L. I., Milev, A. & Usenko, A. *Geophys. J. Int.* **111**, 433–447 (1992).
7. Makeyeva, L. I., Vinnik, L. P. & Roecker, S. W. *Nature* **358**, 144–147 (1992).
8. Hess, H. *Nature* **203**, 629–631 (1964).
9. Blackman, D. K., Orcutt, J. A., Forsyth, D. W. & Kendall, J. M. *Nature* **366**, 675–677 (1993).
10. Raitt, R. W., Shor, G. G. Jr, Francis, T. J. G. & Morris, G. B. *J. geophys. Res.* **74**, 3095–3109 (1969).
11. Zonenshain, L. P. & Savostin, L. A. *Tectonophysics* **76**, 1–45 (1981).
12. Molnar, P. & Tapponnier, P. *Science* **189**, 419–426 (1975).
13. Turcotte, D. L. & Emerman, S. H. *Tectonophysics* **94**, 39–51 (1986).
14. Savage, M. K., Silver, P. G. & Meyer, R. P. *Geophys. Res. Lett.* **17**, 21–24 (1990).
15. Vinnik, L. P., Kosarev, G. L. & Makeyeva, L. I. *Proc. Acad. Sci. U.S.S.R.* **278**, 1335–1339 (1984).
16. Kind, R., Kosarev, G. L., Makeyeva, L. I. & Vinnik, L. P. *Nature* **318**, 358–361 (1985).
17. Silver, P. G. & Chan, W. W. *Nature* **335**, 34–39 (1988).
18. Ansel, V. & Nataf, H. C. *Geophys. Res. Lett.* **16**, 409–412 (1989).
19. Vinnik, L. P., Farra, V. & Romanowicz, B. *Bull. seism. Soc. Am.* **79**, 1542–1558 (1989).
20. Makeyeva, L. I., Plesinger, A. & Horalek, J. *Phys. Earth planet. Inter.* **62**, 298–306 (1990).
21. Silver, P. G. & Chan, W. W. *J. geophys. Res.* **96**, 16429–16454 (1991).
22. Zoback, M. L. *J. geophys. Res.* **97**, 11703–11728 (1992).
23. McNamara, D. E. & Owens, T. J. *J. geophys. Res.* **98**, 12003–12017 (1993).
24. Sheriff, R. E. & Geldart, L. P. *Exploration Seismology* (Cambridge Univ. Press, 1982).
25. Zorin, Yu.A., Yu.A., Kozhevnikov, V. M., Novoselova, M. R. & Turutanov, E. K. *Tectonophysics* **168**, 327–337 (1989).
26. McNamara, D. E., Owens, T. J. & Silver, P. G. *J. geophys. Res.* **99**, 13655–13666 (1994).
27. Sandovol, E., Ni, J., Ozalaybey, S. & Schlue, J. *Geophys. Res. Lett.* **19**, 2337–2340 (1992).
28. Chastel, Y. B., Dawson, P. R., Wenk, H.-R. & Bennett, K. *J. geophys. Res.* **98**, 17757–17771 (1993).

ACKNOWLEDGEMENTS. We thank N. A. Logatchev for his support of this joint preject, and R. Girdler for comments and discussions. We also thank P. Molnar and R. Keller for critical reviews of the manuscript. The REFTEK recorders and some of the seismometers were provided by the PASSCAL Instrument Center at Lamont-Doherty Earth Observatory. Field work in Russia was supported by the Russian Academy of Sciences; work at UCLA and the University of Wisconsin were supported by DARPA.

Multiple processing streams in occipitotemporal visual cortex

Edgar A. DeYoe*, Daniel J. Felleman†‡, David C. Van Essen‡§ & Evelyn McClendon†

* Department of Cellular Biology and Anatomy, The Medical College of Wisconsin, 8701 Watertown Plank Road, Milwaukee, Wisconsin 53226, USA
† Department of Neurobiology and Anatomy, University of Texas Medical School, Houston, Texas 77030, USA
‡ Division of Biology 216–76, California Institute of Technology, Pasadena, California 91125, USA

THE earliest stages of cortical visual processing in areas V1 and V2 of the macaque monkey contain internal subdivisions ('blobs' and 'interblobs' in layer 4B in V1; thin, thick and interstripes in V2) that are selectively interconnected and contain neurons with distinctive visual response properties[1–10]. Here we use anatomical pathway tracing to demonstrate that higher visual areas, V4 and the ventral posterior inferotemporal cortex, each contain anatomical subdivisions that have distinct input and output projections. These findings, in conjunction with others[11–15], suggest that modularity and multistream processing within individual cortical areas are widespread features of neocortical organization.

§ Present address: Department of Anatomy and Neurobiology, Washington University School of Medicine, St Louis, Missouri 63110, USA.

We injected two retrograde tracers (three tracers in one case) into nearby sites in V4 of five hemispheres from three macaque monkeys. For three pairs of injections, strongly segregated clusters of cells labelled by each tracer were found within extrastriate visual areas V2, V3/V3A, V4v/VP and PITv (see legend to Table 1 for abbreviations). Figure 1 illustrates results from one such case (case 1 in Table 1) in which bisbenzimide and nuclear yellow were injected at sites 4.3 mm apart in V4 (Fig. 1*a*). Each injection labelled several bands of cells throughout a 14-mm swath of dorsal V2 (Fig. 1*b*), demonstrating that the two injections involved similar parts of the perifoveal visual field representation. The bisbenzimide was concentrated in the pale-staining interstripes revealed by cytochrome oxidase histochemistry, whereas the nuclear yellow was centred along a subset of the dark cytochrome-oxidase-staining stripes (red outlines in Fig. 1*b*). We infer that the nuclear yellow was primarily in the thin-stripe compartments (even in regions where the pattern was somewhat irregular), because it has been shown elsewhere that (1) the thick stripes do not have a substantial projection to V4 (refs 1, 3, 12, 14) and (2) anatomical segregation is maintained even within regions of irregular stripe geometry[3,14].

The pattern of retrograde labelling in the remainder of extrastriate cortex is shown as a three-dimensional reconstruction of occipitotemporal cortex in Fig. 1*a*, as a single section through the prelunate gyrus in Fig. 1*c*, and as a two-dimensional map of 'unfolded' cortex in Fig. 1*d*. Throughout occipitotemporal cortex, labelled cells were found in clusters of variable shape and size ranging from $\sim 4\ mm^2$ to $>70\ mm^2$.